

# Stability Enhancement of In-Wheel Motor Drive Electric Vehicle Using Adaptive Sliding Mode Control

**Majid Majidi\***

Department of Mechanical Engineering,  
Faculty of Industrial and Mechanical Engineering, Qazvin Branch,  
Islamic Azad University, Qazvin, Iran  
E-mail: m\_majidi@qiau.ac.ir

\*Corresponding author

**Aria Noori Asiabar**

Faculty of Mechanical Engineering,  
K.N. Toosi University of Technology, Tehran, Iran  
E-mail: Aria.noori@email.kntu.ac.ir

**Received: 29 August 2021, Revised: 26 November 2021, Accepted: 05 January 2022**

**Abstract:** A multi-layer controller of direct yaw moment for electric vehicles is developed in this study. In the upper layer, the yaw moment are obtained using Adaptive Sliding Mode Control (ASMC) with adaptation gain to track the desired vehicle yaw rate. The corrective yaw moments are applied by four in-wheel electric motors. The lower layer controller consists of a torque distribution algorithm and in-wheel motor torque controllers as well. The proposed torque distribution algorithm is intended to distribute the reference torques of each in-wheel motor controller appropriately based on both total longitudinal force and corrective yaw moment. To elucidate the effectiveness and robustness of the above control method, the simulation under various manoeuvres was carried out. A 7-DOF non-linear vehicle model is used for simulations and their results signify that the proposed control algorithm accomplishes a proper distribution of longitudinal force among four individual wheels, in turn, enhancing the yaw stability of the vehicle.

**Keywords:** Adaptive Sliding Mode Control, Direct Yaw Moment, Stability Enhancement, Torque Distribution

**How to cite this paper:** Majid Majidi, and Aria Noori Asiabar “Stability Enhancement of In-Wheel Motor Drive Electric Vehicle Using Adaptive Sliding Mode Control”, Int J of Advanced Design and Manufacturing Technology, Vol. 15/No. 2, 2022, pp. 23-33. DOI: 10.30495/admt.2022.1938721.1311.

**Biographical notes:** **Majid Majidi** received his PhD in Automotive Engineering from Iran University of Science and Technology in 2015. He has worked as an assistant professor at Department of Mechanical Engineering, Qazvin Islamic Azad University since 2015. His current research interests include vehicle dynamics, modelling, simulation and control of hybrid and electric vehicles. **Aria Noori Asiabar** received his MSc in vehicle dynamics control from K.N. Toosi University of Technology in 2018. He is currently a PhD student at University of Lincoln working on advanced motion control of articulated vehicles. His research interests include vehicle motion control in theory and applications.

---

## 1 INTRODUCTION

---

Deleterious effects of fossil fuels used in cars with an Internal Combustion Engine (ICE) and increasing public appeal for cutting back weather contamination produced by these cars have drastically expedited the use of cars with zero emissions. Hence, the advancement of Electric Vehicles (EVs) in place of conventional ICE vehicles is growing rapidly. A novel layout used for EVs is to exploit electric motors in the inner space of each wheel. The advantage of using in-wheel motors can be exerted to the design of a control architecture with the point of distributing controlled driving and braking torques independently amongst the wheels of the electric vehicle. The mentioned merit of in-wheel-motor electric vehicles (IWM-EVs) is accompanied by the concentration on stability analysis of these vehicles. Therefore, electric vehicles have been the focus of interest among researchers in recent years [1-2]. The stability problem of EVs under critical manoeuvres is of paramount significance. Hence, the main incentive of this paper lies in the lateral stability enhancement of IWM-EVs. When it comes to vehicle lateral dynamics control, the yaw rate is considered to be the primary control variable [3]. Moreover, the sideslip angle of the vehicle is another control variable kept limited by controlling the vehicle angular velocity of the vehicle in this paper. Thus, a corrective yaw moment generated by the direct yaw moment control (DYC) system is designed to track the desired vehicle yaw rate which in turn keeps the vehicle sideslip angle restricted. In general, DYC systems are categorized into two main systems which are Differential Braking System (DBS) and Torque Vectoring (TV) system which uses asymmetric braking and driving longitudinal forces respectively to create the corrective yaw moment required to maintain the vehicle motion in the desired path [4]. From the point that the driving and braking torques of IWM-EVs can be controlled independently for each wheel, this type of vehicle is the best choice for designing a DYC system. Thereafter, the focus of this paper is to propose a DYC system for IWM-EVs.

A great deal of research on yaw stability control of in-wheel-motor electric vehicles has been largely studied. Yaw stability control of an IWM-EV is mainly realized by independent in-wheel-motor torques control [5-10]. Zhao et al. [11] proposed a sliding model stability control method based on motor drive torque for a four independent in-wheel motor vehicle. However, the motor torque distribution according to the additional yaw moment for stability was not described. Chen et al. proposed three patterns of electric differentials (ED) for four independent in-wheel motor vehicle. However, a vehicle stability control algorithm was not taken into consideration [5]. Xiong et al. proposed quadratic

programming for vehicle stability control to distribute the driving force of the four wheels. However, the regeneration braking force distribution was not analysed [6]. Majidi et al. [7] proposed a vehicle stability enhancement via a combination of direct yaw moment controller with active front steering which is shown to have a better tracking performance compared to single DYC or AFS. Kang et al. proposed a driving control algorithm for a 4WD (4-wheel-driving) EV equipped with independent braking control modules and two-motor torque control to improve vehicle stability [8]. Robust yaw stability control method based on a two-degrees-of-freedom (2-DOF) steering control architecture was presented, and its effectiveness was verified using a hardware-in-the-loop simulation setup [9] and field tests [10]. Kazemi et al. [12-13] used the yaw rate error and the derivative of yaw rate error to achieve the desired yaw moment. In their work, the reference yaw rate is generated through a neural network. Also, in order to prevent the tyre from saturation, they proposed a fuzzy control method in which the slip ratio error and its derivative are fuzzy slip controller inputs. Wang et al. [14] used a robust  $\mu$ -synthesis approach to improve handling stability of a four in-wheel motor electric vehicle. However, this paper took no notice of designing a lower-level controller to realize the additional yaw moment.

In this paper, vehicle stability improvement is achieved through yaw motion control using Adaptive sliding mode control (ASMC) with adaptive gain. This paper presents a hierarchical control approach consisting of an upper controller and a lower controller. The upper controller comprises an adaptive sliding mode control with adaptive gain to generate the corrective yaw moment aimed to follow the desired yaw rate and sideslip angle acquired by the bicycle model. The lower layer controller consists of a torque distribution algorithm and in-wheel motor torque controllers as well. The proposed torque distribution algorithm is intended to distribute the reference torques of each in-wheel motor controller appropriately based on both total longitudinal force and corrective yaw moment. Then, the output torques of in-wheel motor controllers will be given separately to each wheel to generate the desired longitudinal force and consequently yaw moment required to assure the yaw stability.

---

## 2 VEHICLE MODEL

---

In this section, a 7-DOF nonlinear vehicle model involving longitudinal, lateral, and yaw motion in addition to four angular velocities of wheels which are depicted in "Fig.1" is considered. For simplicity in controller design, the roll dynamics is neglected.

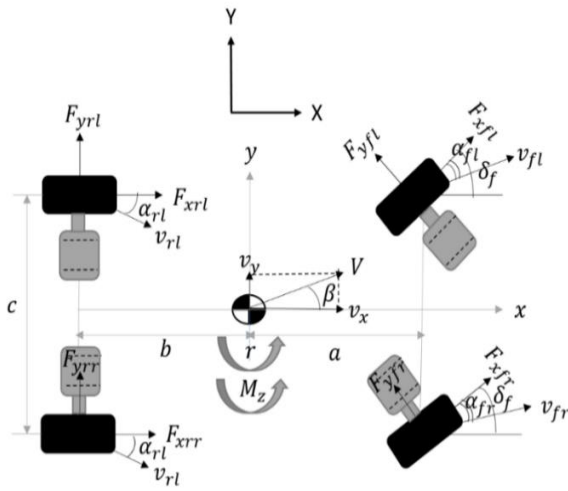


Fig. 1 7-DOF vehicle model.

The differential equations of longitudinal, lateral, and yaw motions are expressed as “Eqs. (1-3)”. These equations are according to Newton’s law of motion:

$$m(\dot{v}_x - r v_y) = (F_{xfl} + F_{xfr}) \cos \delta_f + F_{xrl} + F_{xrr} - (F_{yfl} + F_{yfr}) \sin \delta_f - 0.5c_D A_f \rho_a v_x^2 \quad (1)$$

$$m(\dot{v}_y + r v_x) = (F_{yfl} + F_{yfr}) \cos \delta_f + F_{yrl} + F_{yrr} + (F_{xfl} + F_{xfr}) \sin \delta_f \quad (2)$$

$$I_z \dot{r} = a(F_{yfl} + F_{yfr}) \cos \delta_f - b(F_{yrl} + F_{yrr}) + 0.5c(F_{yfl} - F_{yfr}) \sin \delta_f + M_z \quad (3)$$

In which  $M_z$  is the direct yaw moment and defined as:

$$M_z = a(F_{xfl} + F_{xfr}) \sin \delta_f + 0.5c(F_{xfr} - F_{xfl}) \cos \delta_f + 0.5c(F_{xrr} - F_{xrl}) \quad (4)$$

In above equations,  $m$  is the mass of vehicle;  $a$  and  $b$  are the distances from C.G. to the front and rear axle of the vehicle respectively;  $c$  is the track width;  $I_z$  is the vehicle inertia about the  $z$  axis;  $r$  is the yaw rate;  $\delta_f$  is the front-wheel steer angle,  $F_{xi}$  and  $F_{yi}$  are longitudinal and lateral tyre forces respectively for each wheel. In “Fig. 1”,  $\beta$  is the vehicle body side slip angle defined as the angle between the C.G. velocity vector and the longitudinal axis of the vehicle and it is as follow:

$$\beta = \tan^{-1}(v_y / v_x) \quad (5)$$

The wheel rotational dynamics as shown in “Fig. 2” are described by:

$$I_w \dot{\omega}_i = T_{di} - T_{bi} - F_{xi} R - F_{zi} f_r R_e \quad i = fl, fr, rl, rr \quad (6)$$

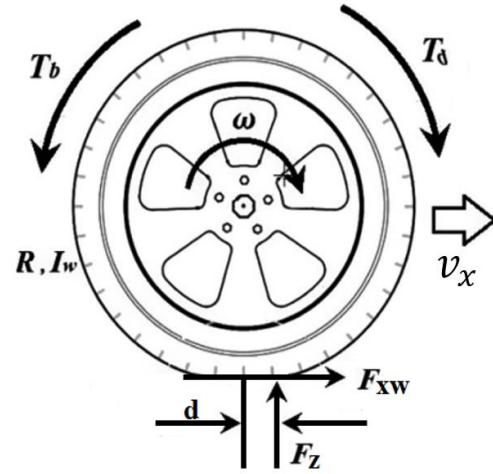


Fig. 2 Free body diagram of wheel rotational dynamics.

Due to the tyre deflection in the contact patch, the normal force does not pass through wheel centre which in turn produces a so-called rolling resistant moment around wheel axis which is denoted by  $f_r$  in “Eq. (6)” where  $T_{di}$  and  $T_{bi}$  denote the driving and braking torques of each wheel respectively,  $\omega_i$  denotes the wheel angular velocity and  $R_e$  denotes the tyre effective radius.

There are many tyre models such as Dugoff model, the Magic Formula, and the Brush model to describe tyre behaviour. A large amount of research has been implemented in the case of tyre modelling and the advantages and drawbacks of each model were discussed. To produce correct tyre forces, a proper tyre model should be provided. Thus, it is of great importance to opt for an appropriate model. One of the most commonly used tyre models in vehicle dynamics simulations was developed by H. Pacejka [15]. Due to the simplicity of the Magic Formula tyre model in describing tyre characteristics based on its physical properties and empirical intrinsic as well, a combined-slip Magic formula (MF) tyre model calculating longitudinal and lateral tyre forces using both longitudinal and lateral slip is employed for tyre modelling. Tyre forces predicted by the Magic Formula method has been proven that are in great conformity with the actual tyre forces [16].

### 3 2-DOF REFERENCE MODEL

Vehicle 2-DOF planar model also named single-track model or bicycle model as shown in “Fig. 3” has been widely used as the reference model for generating the desired value of vehicle yaw angular velocity and also side slip angle. Vehicle lateral dynamics equations can be written as:

$$\begin{aligned} m(\dot{v}_y + r v_x) &= 2F_{yf} + 2F_{yr} \\ I_z \dot{r} &= 2aF_{yf} - 2bF_{yr} \end{aligned} \quad (7)$$

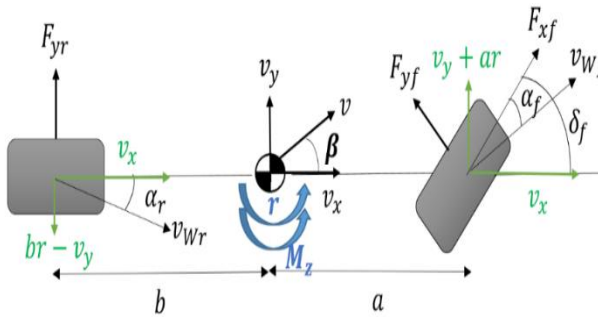


Fig. 3 2-DOF bicycle model.

The desired yaw rate and sideslip angle can be achieved by considering the yaw motion of a vehicle in a steady-state condition.

$$r_{ss} = v_x \delta_f / (l + K_{US} v_x^2) \quad (8)$$

$$\beta_{ss} = (b - (a m v_x^2) / (2l C_{ar})) \delta_f / (l + K_{US} v_x^2) \quad (9)$$

Where  $K_{US}$  is the vehicle understeer gradient and can be described as follows:

$$K_{US} = m (b C_{ar} - a C_{af}) / (2l C_{af} C_{ar}) \quad (10)$$

In “Eq. (10)”,  $C_{af}$  and  $C_{ar}$  are the front and rear tyre cornering stiffness, respectively. It is noteworthy that both the vehicle yaw rate and sideslip angle have the upper bound limited by tyre/road friction coefficient. It means that any amount further than this would not be achievable [4]:

$$r_{max} = (\mu g / v_x) \quad (11)$$

$$\beta_{max} = \tan^{-1}(0.02 \mu g) \quad (12)$$

### 4 CONTROL DESIGN

In this paper, an Adaptive Sliding Mode Control (ASMC) has been adopted as the principal method for realizing the proposed control target. As mentioned earlier, a hierarchical control structure is divided to the upper level, and the lower level is used in the controller design section. Furthermore, the yaw rate of the vehicle in addition to its side slip angle are opted to be control variables guarantying the stability and handling of the vehicle respectively.

The upper-level controller comprises a yaw moment controller using the Adaptive Sliding Mode Control theory to apply the suitable control input so that the system would be stable. The designed control method should provide a corrective yaw moment tracking the desired value of the vehicle yaw rate and consequently maintain the side-slip angle of the vehicle bounded to assure the stability of the vehicle. In this layer, total traction force and yaw moment are calculated and then sent as inputs to the lower level controller section mainly named as the control allocation algorithm. The objective of this section is to allocate the control input as well as the total traction force in terms of torques to four separate in-wheel motor controllers. It is noteworthy that the amounts of these torques must conform to the maximum allowable torque generation of each motor controller. The proposed control allocation is composed of a dynamic load-based torque distribution algorithm exerting the suitable driving and braking torques to the system so that the system stability and handling would be ensured.

A yaw moment controller adopting an adaptive sliding mode control method is proposed to generate desired or corrective yaw moment aiming for stabilizing the vehicle yaw motion and therefore manoeuvrability of the vehicle through exerting differential driving and braking force will be realized. It is absolutely a well-known fact that a sliding mode control theory as a robust control approach is capable of assuring the stability of nonlinear systems or systems with uncertainty and maintain the system insensitive to the uncertainties when trajectories are kept on sliding surface [17].

Considering DYC systems, there are alternative ways to achieve the vehicle stability. The first one is associated with the control of the yaw rate of the vehicle to track the desired yaw rate calculated from the 2DOF vehicle model. The second one is to make sure that the sideslip angle is bounded in its allowable boundary which in turn avoids skidding or spinning. The final approach is pertinent to the combination of those two variables simultaneously in the sliding surface equation as described below [7]:

$$S = r - r_d + \zeta(\beta - \beta_d) \quad (13)$$

As can be seen, there is a weighting factor  $\zeta$  determining the effectiveness of the sideslip angle on the designed sliding surface. Now we consider the vehicle 2-DOF model again to propose a control law:

$$\begin{aligned} m v_x (\dot{\beta} + r) &= 2F_{yf} + 2F_{yr} \\ I_z \dot{r} &= 2aF_{yf} - 2bF_{yr} + M_{zc} \end{aligned} \quad (14)$$

It is obvious that  $M_{zc}$  or corrective yaw moment is the control input aiming for realizing the control objection that is tracking the desired values of vehicle yaw rate and sideslip angle. We aim at stabilizing the vehicle by direct yaw moment control so the steering wheel angle can be considered as a disturbance and the only control input would be the corrective yaw moment. The yaw dynamics equation is rewritten as:

$$\begin{aligned} I_z \dot{r} &= (-2(a^2 C_{af} + b^2 C_{ar}) / v_x) r + 2(bC_{ar} - aC_{af}) \beta \\ &+ 2aC_{af} \delta_f + M_{zc} \end{aligned} \quad (15)$$

And:

$$\begin{aligned} C_{af} &= C_{afn} + \Delta C_{af} \\ C_{ar} &= C_{arn} + \Delta C_{ar} \end{aligned} \quad (16)$$

Where,  $C_{afn}$  and  $C_{arn}$  are nominal values, commonly selected as values for dry asphalt, and  $\Delta C_{af}$ ,  $\Delta C_{ar}$  are variations in parameters that have a physical bound. Considering “Eq. (16)”, the yaw dynamics equation is rewrite as:

$$\begin{aligned} I_z \dot{r} &= (-2(a^2 C_{afn} + b^2 C_{arn}) / v_x) r + \\ &2(bC_{arn} - aC_{afn}) \beta + 2aC_{afn} \delta_f + M_{zc} + d \end{aligned} \quad (17)$$

Where,  $d$  is the following term which we consider as a bounded disturbance:

$$\begin{aligned} d &= (-2(a^2 \Delta C_{af} + b^2 \Delta C_{ar}) / v_x) r + \\ &2(b \Delta C_{ar} - a \Delta C_{af}) \beta + 2a \Delta C_{af} \delta_f \end{aligned} \quad (18)$$

Taking derivative of sliding surface “Eq. (13)”, we have:

$$\dot{S} = \dot{r} - \dot{r}_d + \zeta(\dot{\beta} - \dot{\beta}_d) \quad (19)$$

Then, by substituting “Eq. (17)” in “Eq. (19)” and rewriting the equation,  $\dot{S}$  is obtained as:

$$\begin{aligned} \dot{S} &= (-2a_{1n} / I_z v_x) r + (2a_{2n} / I_z) \beta + (2a_{3n} / I_z) \delta_f \\ &+ (M_{zc} / I_z) + (d / I_z) - \dot{r}_d + \zeta(\dot{\beta} - \dot{\beta}_d) \end{aligned} \quad (20)$$

Where,  $a_{1n}$ ,  $a_{2n}$  and  $a_{3n}$  are as follows:

$$\begin{aligned} a_{1n} &= a^2 C_{afn} + b^2 C_{arn} \\ a_{2n} &= bC_{arn} - aC_{afn} \\ a_{3n} &= aC_{afn} \end{aligned} \quad (21)$$

For designing the conventional sliding mode control [17], the equivalent control input is derived as:

$$\hat{M}_{zc} = \frac{2a_{1n}}{v_x} r - 2a_{2n} \beta - 2a_{3n} \delta_f + I_z \dot{r}_d - I_z \zeta(\dot{\beta} - \dot{\beta}_d) \quad (22)$$

In order to satisfy the sliding condition, a discontinuous term must be added to the corrective yaw moment control law. In sliding mode control theory [17], the discontinuous function gain should be determined in a way that overcomes the uncertainties presenting in the system. For choosing suitable discontinuous function gain, we must know the variation of parameters upper-bound, un-modelled dynamics, the number of noises, etc. But in practice, these values are either unknown or difficult to calculate. One of the alternatives to solve this problem is to select a big enough value for discontinuous function gain. However, this action culminates in a large control signal which is undesirable due to the actuators' limitation issue. One possible method to overcome the mentioned problem is to estimate the discontinuous function gain and to update it through an adaptive mechanism to satisfy the sliding condition. To this aim, to design an ASMC, the constant discontinuous function gain is substituted by a time-varying parameter. Then, corrective yaw moment is obtained as:

$$\begin{aligned} M_{zc} &= 2(a_{1n} / v_x) r - 2a_{2n} \beta - 2a_{3n} \delta_f + I_z \dot{r}_d \\ &- I_z \zeta(\dot{\beta} - \dot{\beta}_d) - \hat{K}_s \sigma I_z \text{sgn}(S) \end{aligned} \quad (23)$$

Where,  $\hat{K}_s$ , the time-varying is estimated discontinuous function gain and  $\sigma$  is a positive constant value. The adaptation mechanism for updating the discontinuous function gain can be:

$$\dot{\hat{K}}_s(t) = S \sigma \text{sgn}(S) \quad (24)$$

The positive constant value,  $\sigma$  determines the adaptation speed of the control gain. Also, the initial condition  $\hat{K}_s$  is considered zero. For designing the control law, the following assumptions should be taken into consideration.

1) The bounded non-negative unknown discontinuous gain  $\hat{K}_s$  exists in such a way that

$$K_s > d_{\max} + \eta \quad , \quad \eta > 0 \quad (25)$$

Where:

$$d_{\max} \geq |d(t)|/I_z \quad \forall t \quad (26)$$

And  $\eta$  is a positive constant value. It should be noted that this condition simply implies that the values of the system's uncertainties must be bounded.

2) The constant value  $\sigma$  must be chosen so that it equals or would be greater than 1 (i.e.  $\sigma \geq 1$ )

Theorem: consider the yaw dynamics represented in "Eq. (15)", if assumptions 1 and 2 are valid, the control law ("Eq. (23)") will result in creating a yaw rate by which the tracking error  $S(t) = r(t) - r_d(t)$  tends to zero when the time tends to infinity. We will prove this theorem through the Lyapunov stability theory.

Proof: Define the Lyapunov function candidate:

$$V = 0.5S(t)S(t) + 0.5\tilde{K}_s(t)\tilde{K}_s(t) \quad (27)$$

And its time-derivative is:

$$\dot{V} = S(t)\dot{S}(t) + \tilde{K}_s(t)\dot{\tilde{K}}_s(t) \quad (28)$$

We know that:

$$\tilde{K}_s(t) = \hat{K}_s(t) - K_s \rightarrow \dot{\tilde{K}}_s(t) = \dot{\hat{K}}_s(t) \quad (29)$$

Considering "Eqs. (20) and (24)", "Eq. (27)" is obtained as:

$$\dot{V} = S(t)\left(\frac{d(t)}{I_z} - \hat{K}_s\sigma \operatorname{sgn}(S)\right) + (\hat{K}_s(t) - K_s)\dot{\hat{K}}_s(t) \quad (30)$$

Also, regarding the "Eq. (24)", "Eq. (30)" takes the following form:

$$\dot{V} = (d(t)/I_z)S(t) - K_s|S(t)|\sigma \quad (31)$$

Using the first assumption, we have:

$$\dot{V} \leq |S|\left\{\left(|d(t)/I_z\right) - (d_{\max} + \eta)\sigma\right\} \quad (32)$$

Considering the first and second assumptions:

$$\dot{V} \leq -\eta|S|\sigma \rightarrow \dot{V} \leq 0 \quad (33)$$

It should be highlighted that the assumptions 1 and 2 are considered in proving this theorem. Employing the Lyapunov's direct method, since  $V(t)$  is a positive-definite function,  $\dot{V}(t)$  is a negative semi-definite function and  $V(t)$  tends to infinity as  $S(t)$  and  $\tilde{K}_s(t)$  tends to infinity. Therefore, the equilibrium at the origin  $[S(t), \tilde{K}_s(t)] = [0, 0]$  would be globally stable, and consequently the variables  $S(t)$  and  $\tilde{K}_s(t)$  will be bounded. Taking the derivative of "Eq. (31)", we have

$$\ddot{V} = \frac{d(t)}{I_z}\dot{S}(t) - K_s\sigma\frac{d}{dt}|S(t)| \quad (34)$$

Due to the boundness of  $\dot{S}$ ,  $\ddot{V}$  is deduced to be bounded.  $\dot{V}$  is a uniformly continuous function. Therefore, in terms of Barbalat's lemma, it will be proved that  $\dot{V}(t) \rightarrow 0$  when  $t \rightarrow \infty$  which means that  $S(t) \rightarrow 0$  when  $t \rightarrow \infty$  and the system would be asymptotically stable.

The control law (23) is in a discontinuous manner which in turn causes chattering due to the measuring noise and actuator delay. Designing of conventional sliding mode control methods requires the knowledge of the upper-bound of the system's uncertainties because this upper-bound is used in discontinuous function gain computation. Therefore, the upper-bound of uncertainties must be determined in high precision since the higher the upper-bound uncertainties is, the more values of discontinuous function gain we need to overcome the uncertainties which in turn requires higher control effort, in other words, high activity of actuators which is undesirable in practice. To resolve this unwanted problem, in this paper, an adaptive rule is employed to calculate discontinuous function gain ( $K_s$ ) aiming at the lacking necessity for uncertainties upper-bound calculation. This problem can be solved through the substitution of the discontinuous term (i.e.  $\operatorname{sgn}(S)$ ) with the saturation function with the boundary layer thickness of  $\phi$  as a continuous approximation of the function  $\operatorname{sgn}(S)$ :

$$\text{sgn}(S) \approx \text{sat}(S / \phi) = \begin{cases} (S / \phi) & \text{if } |(S / \phi)| < 1 \\ \text{sgn}(S / \phi) & \text{otherwise} \end{cases} \quad (35)$$

Therefore, we create a continuous approximation of a discontinuous sliding mode control law within the boundary layer which guarantees the movement along the sliding surface. Although using saturation function instead of sign function causes the chattering phenomenon to be diminished, the tracking performance would be deteriorated. By regulating the boundary layer thickness, there would be a compromise between the chattering phenomenon and the tracking error. In other words, if the thickness of the boundary layer is chosen some value around zero, then the designed controller acts as a conventional sliding mode control with sign function which signifies the high chattering and the less tracking error. On the contrary, when the thickness of the boundary layer is big enough, the chattering phenomenon would die away and the tracking performance would be deteriorated severely in return.

## 5 TORQUE DISTRIBUTION ALGORITHM

The generated corrective yaw moment in addition to the total traction force should be allocated to four in-wheel motor controllers with the duty of realizing the driving or braking torques they receive from the control allocation algorithm. Furthermore, these driving and braking motor torques are employed separately at each motor to provide the calculated corrective yaw moment so that it could track the desired value of defined variables and as a consequence, the stability of the vehicle will be achieved; Hence, it can be grasped that the yaw stability of a vehicle will be realized through individually monitoring the driving and braking forces of each wheel produced by every one of in-wheel motors. In this study, an equal-load- based torque distribution strategy is proposed to distribute the amounts of yaw motion and total traction force in terms of four driving and braking torques to each in-wheel motor controllers. This strategy is employed to allocate the total traction force and corrective yaw moment, which is computed from the upper layer, equally to four in-wheel motors. The total amount of traction force is described as follows:

$$F_{xt} = F_{xfl} + F_{xfr} + F_{xrl} + F_{xrr} \quad (36)$$

$$(F_{xfl} / F_{xrl}) = \rho_L = 1 \quad , \quad (F_{xfr} / F_{xrr}) = \rho_R = 1 \quad (37)$$

By considering “Fig. 1” and a small value of  $\delta_f$ , that is,  $\sin \delta_f \approx 0$  and  $\cos \delta_f \approx 1$ , the corrective yaw moment will be:

$$M_{zc} = 0.5c (-F_{xfl} + F_{xfr} - F_{xrl} + F_{xrr}) \quad (38)$$

The traction force of four wheels are obtained using “Eqs (36-38)” as follows:

$$F_{xfr} = F_{xrr} = (F_{xt} / 4) + (M_{zc} / (2c)) \quad (39)$$

$$F_{xfl} = F_{xrl} = (F_{xt} / 4) - (M_{zc} / (2c)) \quad (40)$$

Then the desired torques applied to four motor controllers for generating obtainable torques for four in-wheel electric motors can be considered as:

$$T_{fr,des} = R_e F_{xfr} = (F_{xt} R_e / 4) + (M_{zc} R_e / (2c)) \quad (41)$$

$$T_{rr,des} = R_e F_{xrr} = (F_{xt} R_e / 4) + (M_{zc} R_e / (2c)) \quad (42)$$

$$T_{fl,des} = R_e F_{xfl} = (F_{xt} R_e / 4) - (M_{zc} R_e / (2c)) \quad (43)$$

$$T_{rl,des} = R_e F_{xrl} = (F_{xt} R_e / 4) - (M_{zc} R_e / (2c)) \quad (44)$$

## 6 SIMULATION RESULTS

Two manoeuvres, including lane change and step-steer, are carried out through MATLAB/Simulink simulation in different road conditions to demonstrate the effectiveness of the proposed control structure. Vehicle parameters for simulation are shown in “Table 1”. The first simulation relates to lane change on a low friction road. The manoeuvre is at 80 km/h on a low friction road where the friction coefficient is 0.3. The front wheels steering angle is shown in “Fig. 4”.

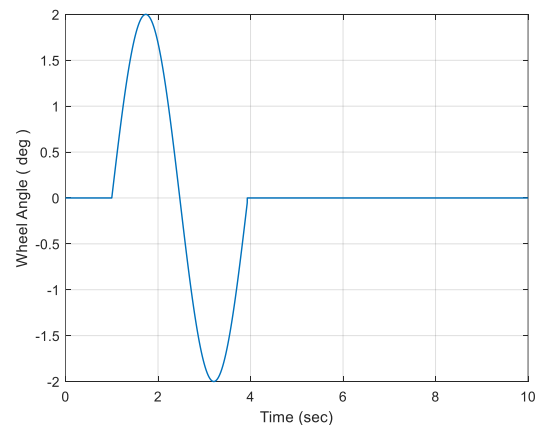


Fig. 4 Front wheels’ steer angle in lane change manoeuvre on low friction road.

The simulation results are shown in “Figs. 5 to 9”. The simulation is done with and without the proposed

controller to examine the controller performance. Figure 5 shows the vehicle yaw rate tracking performance.

**Table 1** Vehicle Parameters

Description	symbol	Unit	Value
Vehicle mass	$m$	kg	1411
Yaw moment of inertia	$I_z$	kgm <sup>2</sup>	2031.4
Height of C.G.	$h$	m	0.54
Distance from C.G. to front axle	$a$	m	1.56
Distance from C.G. to rear axle	$b$	m	1.04
Wheelbase	$l$	m	2.06
Axle track	$c$	m	1.48
Motor resistance	$R_m$	$\Omega$	0.3
Motor inductance	$L_m$	H	0.003
Maximum motor power	$p_{\max}$	kW	25
Maximum motor torque	$T_{\max}$	Nm	320
Drag coefficient	$C_d$	–	0.45
Air density	$\rho_a$	kg/m <sup>3</sup>	1.1
Frontal area	$A_f$	m <sup>2</sup>	2
Front tyre cornering stiffness	$C_{\alpha f}$	N/rad	37407
Rear tyre cornering stiffness	$C_{\alpha r}$	N/rad	51918
Tyre effective radius	$R_e$	m	0.3
Tyre moment of inertia	$J_w$	kgm <sup>2</sup>	2.46
Rolling resistance coefficient	$f_r$	–	0.02

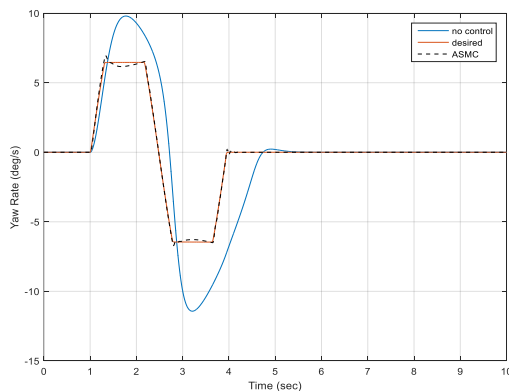


**Fig. 5** Vehicle yaw rate in lane change manoeuvre on low friction road.

From “Fig. 6”, it can be seen that the uncontrolled vehicle acceleration peaked at its maximum value, while in the vehicle with the proposed controller, the lateral acceleration behaves according to driver steering angle request.

As illustrated in “Fig. 7”, the vehicle sideslip angle is kept limited using sliding mode control with gain adaptation. Also, driving and braking torques are illustrated in “Fig. 8”. Negative torques indicate regenerative braking. As one can see, with the use of the proposed controller the state variables are kept in the safe region compared to uncontrolled vehicle. Besides, as represented in “Fig. 9”, the ideal lateral displacement is gained after a longitudinal displacement of 60 meters, while the uncontrolled vehicle failed to return to the intended path, causing deviation from the intended path.

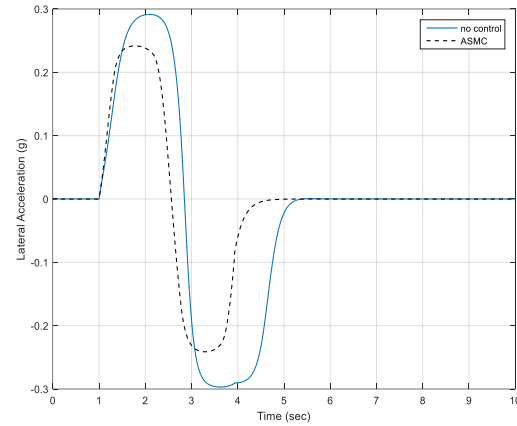


**Fig. 6** Vehicle lateral acceleration in lane change manoeuvre on low friction road.

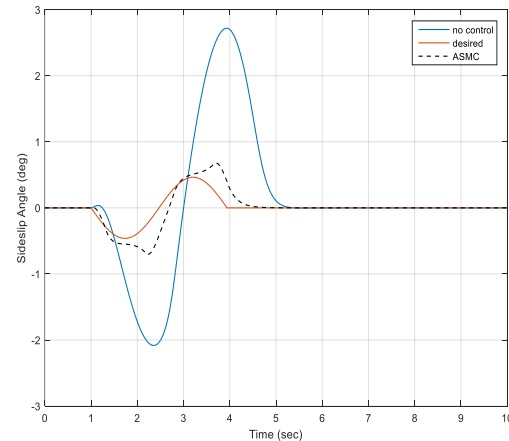


**Fig. 7** Vehicle sideslip angle in lane change manoeuvre on low friction road.

The second simulation is pertinent to step-steer on a dry road. The manoeuvre is at 90 km/h on a high friction road where the friction coefficient is 0.8. The front wheels steer angle is shown in “Fig. 10”. The simulation results are shown in “Figs. 10 to 14”. From figures, one can deduce that the controller tries to limit the sideslip angle in a good way and that the tracking performance

for yaw rate is very satisfying which in turn leads to vehicle handling improvement.

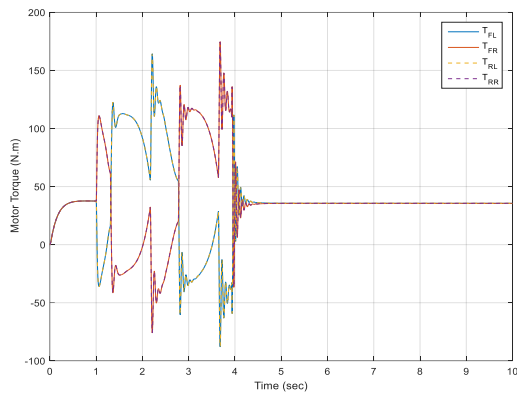


**Fig. 8** Four driving/braking torques of each wheel in lane change manoeuvre on low friction road.

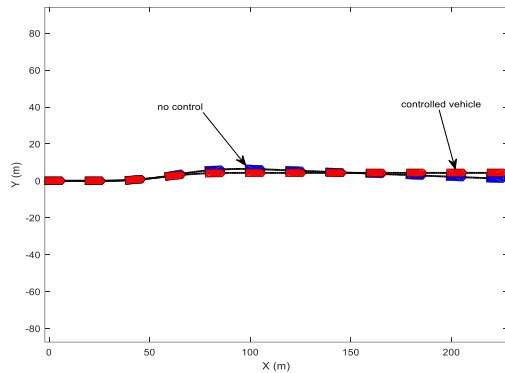


**Fig. 9** Vehicle path in lane change manoeuvre on low friction road.

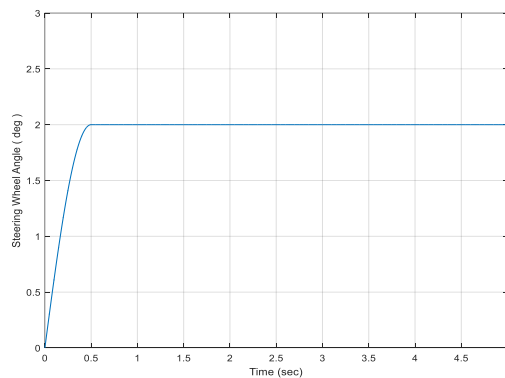


**Fig. 10** Front wheels' steer angle in step-steer on a dry road.

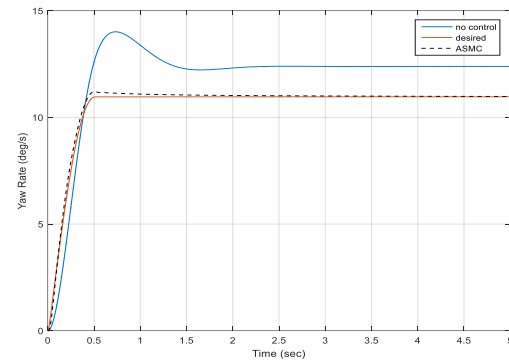


**Fig. 11** Vehicle yaw rate in step-steer on a dry road.

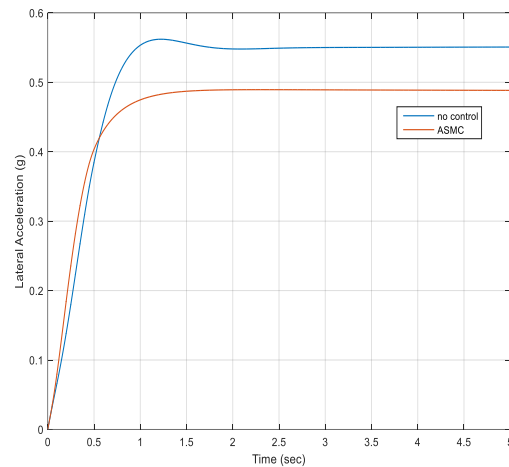


**Fig. 12** Vehicle lateral acceleration in step-steer on a dry road.

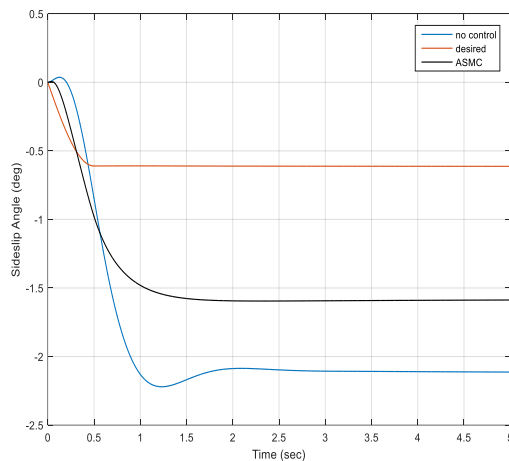


**Fig. 13** Vehicle sideslip angle in step-steer on a dry road.

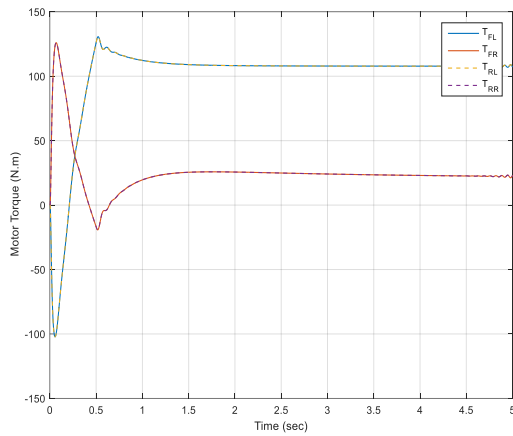


Fig. 14 Four driving/braking torques of each wheel in step-steer on a dry road.

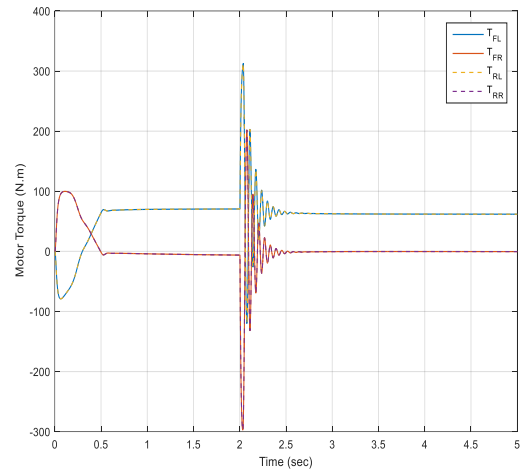


Fig. 17 Four driving/braking torques of each wheel in sudden entrance into a low friction road.

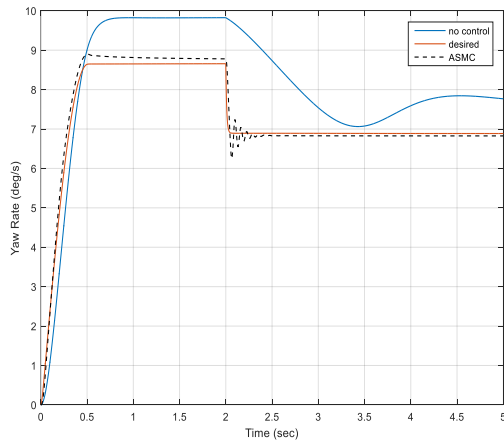


Fig. 15 Vehicle yaw rate in sudden entrance into a low friction road.

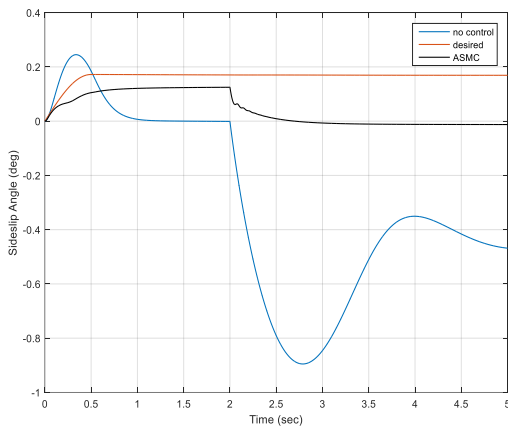


Fig. 16 Vehicle sideslip angle in sudden entrance into a low friction road.

In the third simulation, the vehicle enters from a high-friction road into a low-friction surface suddenly. Moreover, the initial speed of the vehicle is 50 k m/h . The simulation results are shown in “Figs. 15 to 17”. Similar to two earlier simulations, the vehicle yaw rate tracks its desired value in a fairly precise manner as shown in “Fig. 15”. Furthermore, the vehicle sideslip angle is maintained limited in “Fig. 16” thanks to ASMC employment. According to the simulation results, it can be found that, in terms of changing the road friction coefficient, the proposed ASMC with torque distribution has a significantly impressive effect on vehicle handling stability.

## 7 CONCLUSION

In this paper, an adaptive sliding mode controller with gain adaptation is used to enhance the stability of the vehicle. Also, an equal-load- based torque distribution strategy is employed to distribute the virtual controls to driving or braking torques of hub motors. MATLAB/Simulink is used to simulate the model equations. In terms of simulation results, it can be seen that the tracking performance of the yaw rate is improved and the sideslip angle of the vehicle is kept limited aiming at vehicle handling stability improvement. The main contributions of this paper are the use of gain adaptation in the sliding mode control framework and the fuzzy control rule for the discontinuous term in control law to handle the chattering phenomenon.

## REFERENCES

- [1] Khajepour, A., Fallah, M. S., and Goodarzi, A., *Electric and Hybrid Vehicles: Technologies, Modeling and Control-a Mechatronic Approach*, John Wiley & Sons, New Jersey, USA, 2014, ISBN: 1118341511.
- [2] Murata, S., *Innovation by in-Wheel-Motor Drive Unit, Vehicle System Dynamics*, Vol. 50, No. 6, pp. 807-830, 2012, DOI: 10.1080/00423114.2012.666354.
- [3] Wong, J. Y., *Theory of Ground Vehicles*, John Wiley & Sons, 2008, ISBN: 0470170387.
- [4] Rajamani, R., *Vehicle Dynamics and Control*, Springer Science & Business Media, 2011, ISBN: 1461414326.
- [5] Chen, X., Gu, C., Yin, J., Tang, F., and Wang, X., *An Overview of Distributed Drive Electric Vehicle Chassis Integration*, Proceedings of 2014 IEEE Conference and Expo Transportation Electrification Asia-Pacific, IEEE, Beijing, China, 2014, pp.1-5, DOI: 10.1109/ITEC-AP.2014.6940667.
- [6] Xiong, L., Yu, Z., *Control Allocation of Vehicle Dynamics Control for a 4 in-Wheel-Motored Ev*, Proceedings of 2nd International Conference on Power Electronics and Intelligent Transportation System (PEITS), Vol. 2, IEEE, Shenzhen, China, 2009, pp. 307-311, DOI: 10.1109/PEITS.2009.5406779.
- [7] Mashadi, B., Majidi, M., *Integrated Afs/Dyc Sliding Mode Controller for a Hybrid Electric Vehicle*, International Journal of Vehicle Design, Vol. 56, No. 1-4, pp. 246-269, 2011, DOI: 10.1504/IJVD.2011.043268.
- [8] Kang, J., Yoo, J., and Yi, K., *Driving Control Algorithm for Maneuverability, Lateral Stability, and Rollover Prevention of 4wd Electric Vehicles with Independently Driven Front and Rear Wheels*, IEEE Transactions on vehicular technology, Vol. 60, No. 7, pp. 2987-3001, 2011, DOI: 10.1109/TVT.2011.2155105.
- [9] Guvenc, B. A., Guvenc, L., and Karaman, S., *Robust Yaw Stability Controller Design and Hardware-in-the-Loop Testing for a Road Vehicle*, IEEE Transactions on Vehicular Technology, Vol. 58, No. 2, pp. 555-571, 2008, DOI: 10.1109/TVT.2008.925312.
- [10] Nam, K., Kim, Y., Oh, S., and Hori, Y., *Steering Angle-Disturbance Observer (Sa-Dob) Based Yaw Stability Control for Electric Vehicles with in-Wheel Motors*, Proceedings of ICCAS 2010, IEEE, Gyeonggi-do, South Korea, 2010, pp. 1303-1307, DOI: 10.1109/ICCAS.2010.5670238.
- [11] Zhao, Y. E., Zhang, J. W., *Stability Control for a Four-Motor-Wheel Drive Electric Vehicle Based on Sliding Mode Control*, Journal of Shanghai Jiaotong University, Vol. 10, pp. 1526-1530, 2009, DOI: 10.1109/FSKD.2009.582.
- [12] Tahami, F., Kazemi, R., and Farhanghi, S., *A Novel Driver Assist Stability System for All-Wheel-Drive Electric Vehicles*, IEEE Transactions on vehicular Technology, Vol. 52, No. 3, pp. 683-692, 2003, DOI: 10.1109/TVT.2003.811087.
- [13] Tahami, F., Farhanghi, S., and Kazemi, R., *A Fuzzy Logic Direct Yaw-Moment Control System for All-Wheel-Drive Electric Vehicles*, Vehicle System Dynamics, Vol. 41, No. 3, pp. 203-221, 2004, DOI: 10.1076/vesd.41.3.203.26510.
- [14] Yin, G., Wang, R., and Wang, J., *Robust Control for Four Wheel Independently-Actuated Electric Ground Vehicles by External Yaw-Moment Generation*, International Journal of Automotive Technology, Vol. 16, No. 5, pp. 839-847, 2015, DOI: 10.1007/s12239-015-0086-2.
- [15] Bakker, E., Nyborg, L., and Pacejka, H. B., *Tyre Modelling for Use in Vehicle Dynamics Studies*, SAE Transactions, Vol. 96, pp. 190-204, 1987, DOI: 10.4271/870421.
- [16] Pacejka, H., Besselink, I., *Magic Formula Tyre Model with Transient Properties*, Vehicle system dynamics, Vol. 27, No. S1, pp. 234-249, 1997, DOI: 10.1080/00423119708969658.
- [17] Slotine, J. J. E., Li, W., *Applied Nonlinear Control*, Prentice hall, Englewood Cliffs, NJ, USA, 1991, ISBN: 0130408905.